Supporting Information

Tracking the Superefficient Anion Exchange of a Dynamic Porous Material Constructed by Ag(I) Nitrate and Tripyridyltriazole *via* Multi-Step Single-Crystal-To-Single-Crystal Transformations

Cheng-Peng Li,[†] Bo-Lan Liu,[†] Lei Wang,[†] Yue Liu,[†] Jia-Yue Tian,[‡] Chun-Sen Liu[*,‡] and Miao Du[*,†,‡]

[a] *College of Chemistry, Tianjin Normal University, Tianjin 300387, P. R. China*

[b] *Henan Provincial Key Laboratory of Surface & Interface Science, Zhengzhou University of Light Industry, Zhengzhou 450002, P. R. China*

E-mail: dumiao@public.tpt.tj.cn; chunsenliu@zzuli.edu.cn

General Materials and Methods

The L^{243} ligand was similarly prepared according to the literature method (*Eur. J. Org. Chem.* **2004**, 3422–3434) and all other chemicals were obtained commercially. Deionized water was employed throughout the experiments. Elemental analysis for C, H, and N was performed on a Vario EL III Elementar analyzer. IR spectra were taken on a Bruker Tensor 27 OPUS FT-IR spectrometer (with KBr pellet) in 4000–400 cm^{-1}. Powder X-ray diffraction (PXRD) patterns were taken on a Rigaku model Ultima IV diffractometer with Rigaku D/teX ultrahigh-speed position sensitive detector and Cu-Kα X-ray (40 kV and 100 mA), in a step-scan mode with the scan rate of 2 °/min and step size of 0.02°. Simulation of PXRD patterns was carried out using single-crystal diffraction data with the diffraction-crystal module of *Mercury* program. UV-Vis spectra were recorded on a PerkinElmer Lambda 35 spectrophotometer. Inductively coupled plasma mass spectroscopy (ICP-MS) analysis was conducted using a Perkin-Elmer ELAN 9000 instrument after degradation of the sample in HNO_3.

Synthesis of 3-(2-Pyridyl)-4-(4-Pyridyl)-5-(3-Pyridyl)-1,2,4-Triazole (L^{243})

A mixture of 4-aminopyridine (9.31 g, 0.10 mol), sulfur (9.62 g, 0.30 mol), and sodium sulfide nonahydrate (0.48 g, 2 mol %) in 2-methylpyridine (60 mL) was refluxed for 48 h. After cooling and removing all volatiles in vacuo, the dark solid residue was treated with a water solution of sodium hydroxide (2 M, 200 mL) and then filtered. The filtrate was diluted with water (400 mL) and acidified to pH 5 by dropwise addition of concentrated hydrochloric acid. The resulting yellow precipitate was filtered off and washed thoroughly with water. Drying in vacuo will produce analytically pure *N*-(4-pyridyl)pyridine-2-thiocarboxamide (**1**) as a yellow powder in 84% yield (18.2 g). M. p. 130–132 °C. A mixture of **1** (3.00 g, 14.0 mmol) and nicotinohydrazide (2.30 g, 17.0 mmol) in 1-butanol (80 mL) was refluxed for 24 h. Upon cooling, the product will crystallize from the orange reaction mixture, which was filtered

off, washed with ethanol and dried in vacuo to afford L^{243} as colorless needle crystals. Yield: 3.20 g (76%). M. p. 235–237 °C.

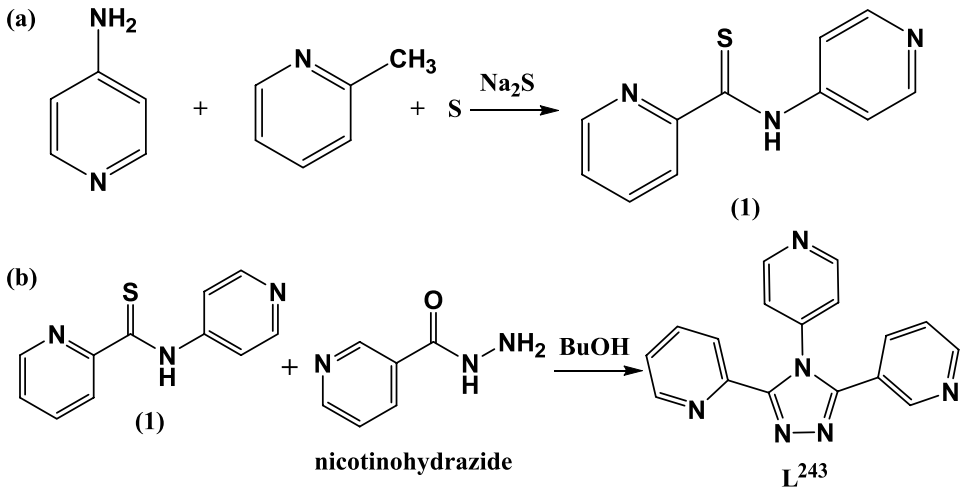

Scheme S1. Synthetic procedure of (a) *N*-(4-pyridyl)pyridine-2-thiocarboxamide and (b) L^{243} ligand.

Synthesis of $[Ag(L^{243})](NO_3)(H_2O)(CHCN_3)$ ($1{\cdot}NO_3$)

A CH_3CN solution (4 mL) of the L^{243} ligand (30.1 mg, 0.1 mmol) was carefully layered on a buffer of ethyl acetate (4 mL), below which a water solution (4 mL) of $AgNO_3$ (17.0 mg, 0.1 mmol) was placed in a straight glass tube. The tube was left to stand at room temperature in darkness. Colorless block crystals for **$1{\cdot}NO_3$** were collected after ca. three days in 85% yield (45.2 mg). Elemental analysis (calcd) for $C_{19}H_{17}AgN_8O_4$: C 43.12, H 3.24, N 21.17%; found: C 42.78, H 3.46, N 21.28%.

Anion Exchange Capacity

Molar Ratio 1 : 1 at 298 and 353 K. The crushed microcrystalline solid of **$1{\cdot}NO_3$** (52.9 mg, 0.1 mmol) was immersed into an aqueous solution (10 mL) of $KMnO_4$ (15.8 mg, 0.1 mmol), which was left to stand at room temperature (298 K) or temperature chamber (353 K). Both solution and solid were monitored at different time intervals to follow the process for anion

exchange with UV-Vis and ICP-MS, respectively. As for UV-Vis measurement, the $KMnO_4$ solution (0.1 mL) was pipetted at different time intervals and diluted with deionized water (2 mL). The anion exchange capacity for **1·NO$_3$** was evaluated by measuring the decolorization rate of $KMnO_4$ solution according to Beer's Law. Notably, the sample for ICP-MS should be carefully washed with deionized water for at least three times to avoid any adherent $KMnO_4$ on crystal surface.

Molar Ratios 2 : 1 and 4 : 1 at 298 and 353 K. The same procedure was applied except by adding the double **1·NO$_3$** (105.8 mg, 0.2 mmol) or quadruple **1·NO$_3$** (211.6 mg, 0.4 mmol) into the initial water solution of $KMnO_4$.

Shortest Time of Adsorption Saturation for 1·NO$_3$

As-synthesized **1·NO$_3$** (0.1 mmol) powders were immersed into a water solution (25 mL) of saturated $KMnO_4$ (ca. 0.4 M), and this mixture (**1·NO$_3$** : $KMnO_4$ = 1 : 100) was left to stand at room temperature. Upon completion, the solid was collected by filtration and washed with water several times, which was characterized by PXRD and FT-IR.

Detection Limit

As-synthesized **1·NO$_3$** (0.2 mmol) powders were immersed into a water solution (10 mL) of saturated $KMnO_4$ (1 ppm) and then left to stand at room temperature. Upon completion, the solid was filtered out and the solution was characterized by UV-Vis and ICP-MS.

Anion-Exchange Selectivity

As-synthesized **1·NO$_3$** (0.1 mmol) powders were immersed into the mixture solution (10 mL) of $KMnO_4$ (0.1 mmol) and KX salt (X = CrO_4^{2-}, SO_4^{2-}, $CF_3SO_3^-$, ClO_4^-, BF_4^-, and $Cr_2O_7^{2-}$) of each at room temperature for 48 h. Upon completion, the solid was collected by filtration and washed with water several times, which was characterized by PXRD and FT-IR.

Single-Crystal X-Ray Diffraction

Single-crystal X-ray diffraction data for all the phases were collected on an Oxford Xcalibur Gemini Eos diffractometer with graphite-monochromated Mo-Kα radiation (λ = 0.71073 Å) at 294(2) K. Multi-scan absorption corrections were performed by the *CrysAlisPro* program and empirical absorption corrections were taken with spherical harmonics implemented with *SCALE3 ABSPACK* scaling algorithm. The crystal structures were solved by direct methods, and all non-hydrogen atoms were refined anisotropically by full-matrix least-squares method with the *SHELXTL* crystallographic software package. H atoms of water in **1·NO$_3$** were first located in the difference maps and then allowed to ride on the parent atoms for refinements. All other hydrogen atoms were located in calculated positions and treated in the subsequent refinement as riding. The disorder nitrate and permanganate in **3·NO$_3$·MnO$_4$** were located on the same site with 0.16 and 0.84 occupancy, respectively. Standard geometry constraint was used for nitrate anion to improve the refinement stability, on which the *FLAT* constraint was also imposed. All non-H atoms for acetonitrile, nitrate, and permanganate were refined with pseudo-isotropic *ISOR* restraint and similar U_{ij} (*SIMU*) restraint, because the free refinement will result in unrealistic anisotropic displacement parameters. Rigid bond (*DELU*) restraint was also applied to treat these atoms. In the structures of **3·NO$_3$·MnO$_4$** and **4·MnO$_4$**, the lattice acetonitrile was assigned to half occupancy to achieve the appropriate thermal parameters. Further crystallographic data and structural refinement details are shown in Table S1.

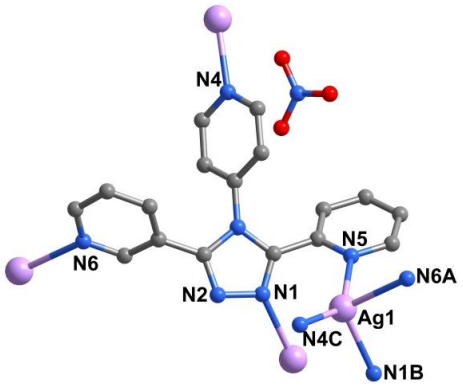

(a)

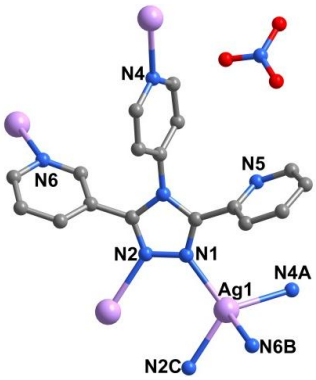

(b)

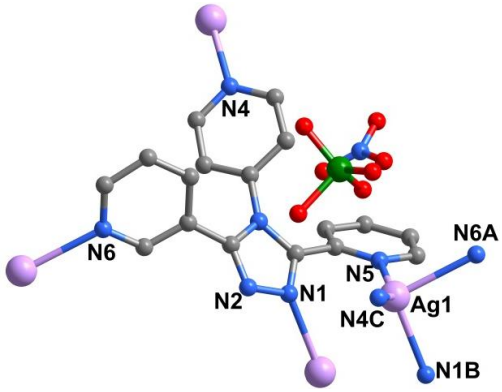

(c)

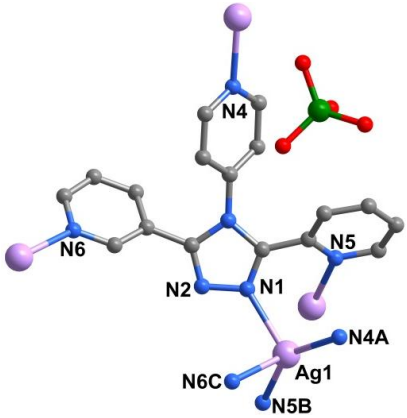

(d)

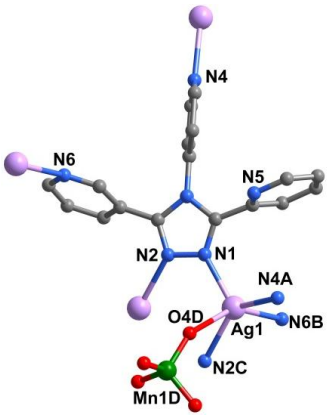

(e)

Figure S1. Local crystal structures for (a) **1·NO_3**, (b) **2·NO_3**, (c) **3·NO_3·MnO_4**, (d) **4·MnO_4** and (e) **5·MnO_4**. Symmetry codes for (a): A = –1 + *x*, *y*, *z*; B = 1 – *x*, 2 – *y*, –*z*; C = 3/2 – *x*, 1/2 + *y*, 1/2 – *z*. For (b): A = –1/2 + *x*, 1/2 – *y*, 1/2 + *z*; B = –1 + *x*, *y*, *z*; C = –*x*, –*y*, 1 – *z*. For (c): A = 1 + *x*, *y*, *z*; B = 1 – *x*, 1 – *y*, 1 – *z*; C = 1/2 – *x*, 1/2 + *y*, 1/2 – *z*. For (d): A = –1/2 + *x*, 1/2 – *y*, 1/2 + *z*; B = 1 – *x*, –*y*, –*z*; C = 2 – *x*, –*y*, –*z*. For (e): A = –1 + *x*, –1/2 – *y*, –1/2 + *z*; B = –1 + *x*, *y*, *z*; C = –*x*, –1 – *y*, 1 – *z*; D = –*x*, –1/2 + *y*, 1/2 – *z*.

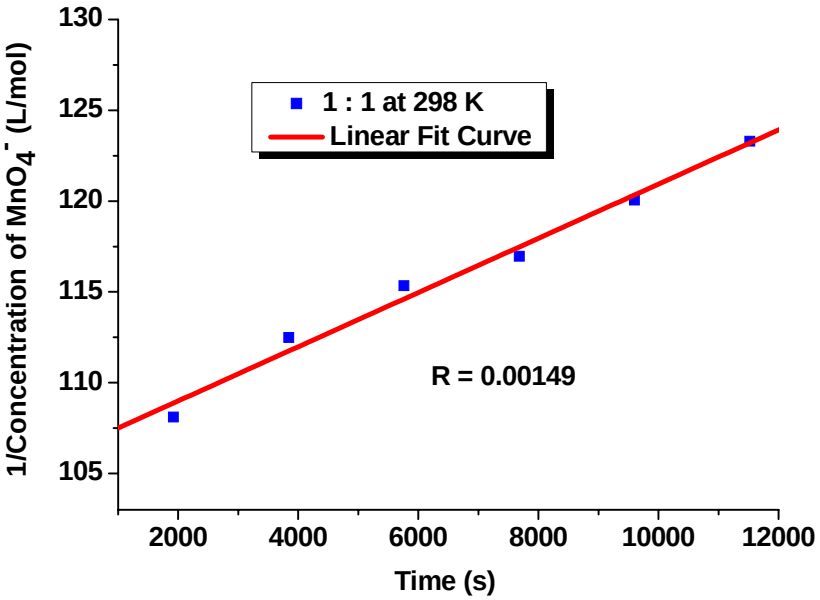

(a)

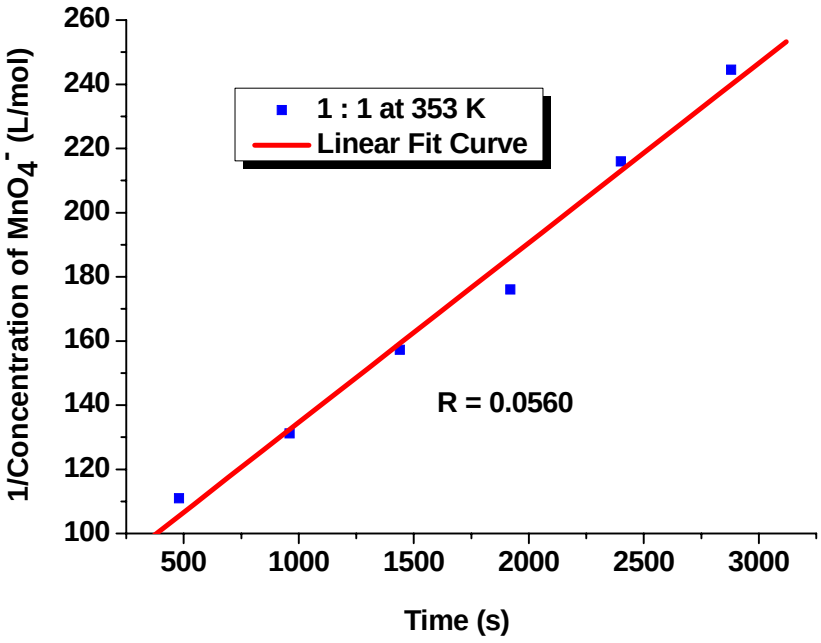

(b)

Figure S2. Kinetic curve of anion exchange with **1·NO$_3$** at (a) 298 and (b) 353 K: plot of 1/concentration of MnO_4^- as a function of time. Parameters for linear fitting: (a) Adj. R^2 = 0.9841, slope = 0.00149 ± 9.37 $\times 10^{-5}$ $s^{-1} \cdot M^{-1}$; (b) Adj. R^2 = 0.99345, slope = 0.056 ± 3.22 $\times 10^{-3}$ $s^{-1} \cdot M^{-1}$.

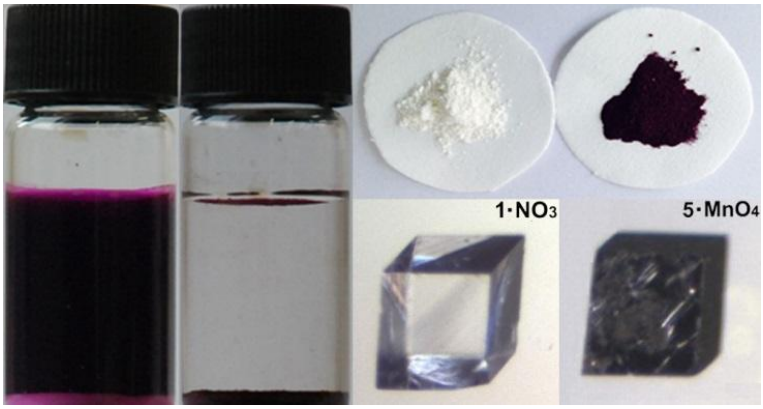

(a)

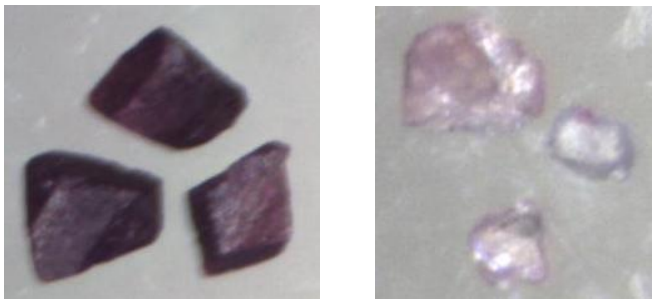

(b)

Figure S3. (a) Photos of the initial and terminal states for anion exchange reaction in solution as well as microcrystalline powders and large single crystals for **1·NO$_3$** and **5·MnO$_4$** samples. (b) Photos of the **2·NO$_3$** crystals as well as their transparent inner cores after taking off the black surface.

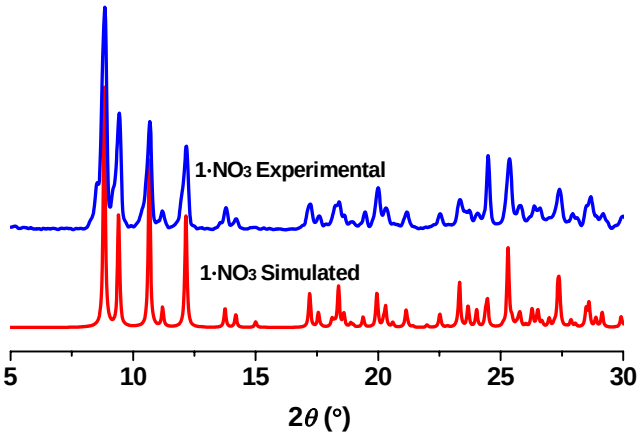
1·NO3 Experimental
1·NO3 Simulated
5
10
15
20
25
30
2θ (°)

(a)

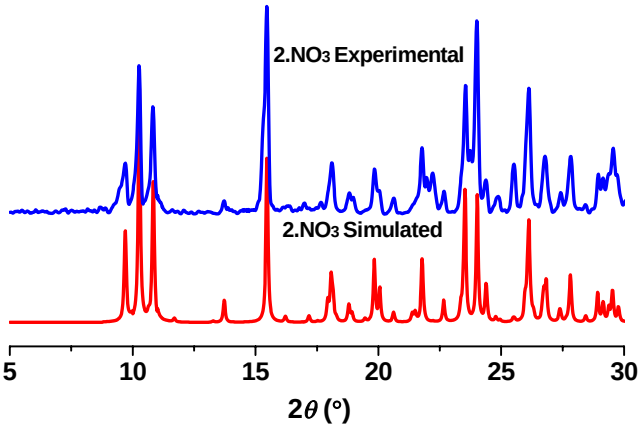
2.NO3 Experimental
2.NO3 Simulated
5
10
15
20
25
30
2θ (°)

(b)

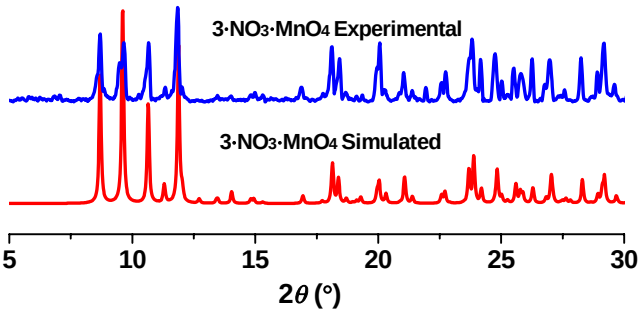
3·NO3·MnO4 Experimental
3·NO3·MnO4 Simulated
5
10
15
20
25
30
2θ (°)

(c)

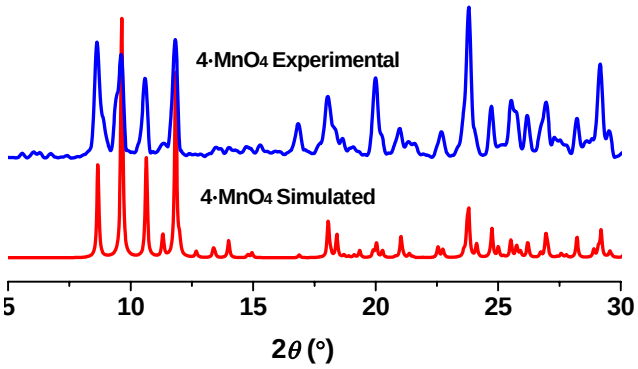

(d)

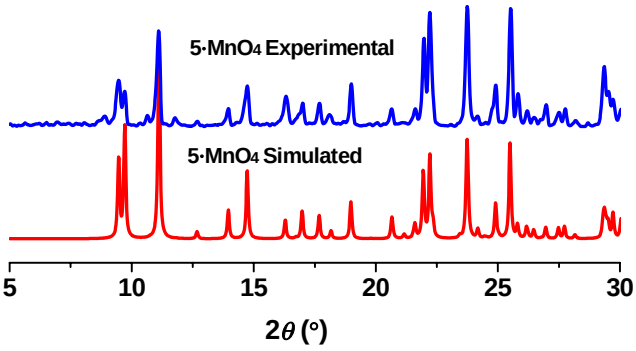

(e)

Figure S4. Powder X-ray diffraction (PXRD) patterns for (a) **1·NO$_3$**, (b) **2·NO$_3$**, (c) **3·NO$_3$·MnO$_4$**, (d) **4·MnO$_4$** and (e) **5·MnO$_4$**. Notably, **3·NO$_3$·MnO$_4$** and **4·MnO$_4$** are always concomitant. The samples for PXRD and FT-IR characterization (Figure S6) were obtained by a collection of their respective single crystals, each of which was confirmed by single-crystal X-ray diffraction (SC-XRD).

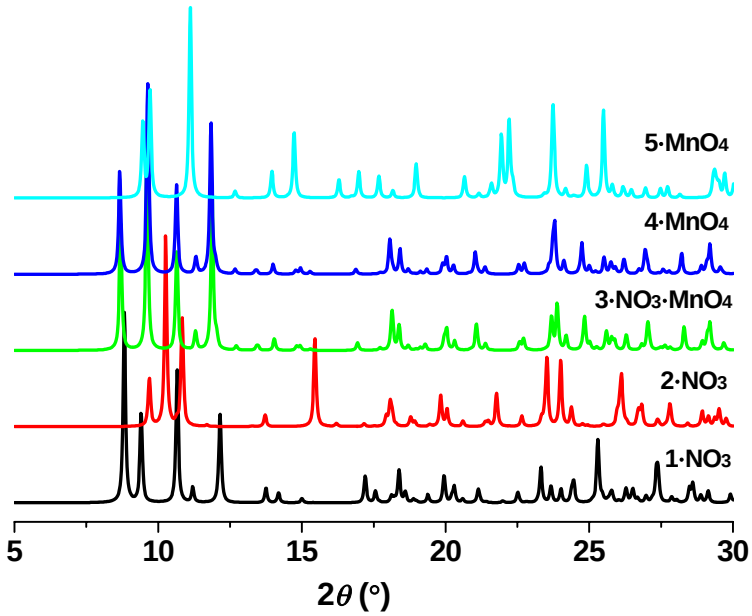

Figure S5. Comparison of the PXRD patterns for **1·NO_3**, **2·NO_3**, **3·NO_3·MnO_4**, **4·MnO_4** and **5·MnO_4**.

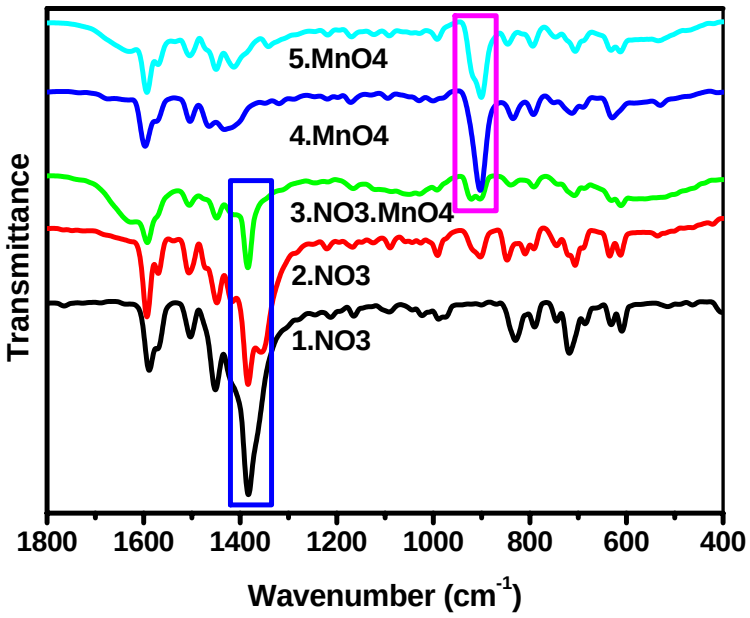

Figure S6. Comparison of the FT-IR spectra for **1·NO_3**, **2·NO_3**, **3·NO_3·MnO_4**, **4·MnO_4** and **5·MnO_4**, highlighting the characteristic peaks of nitrate and permanganate anions.

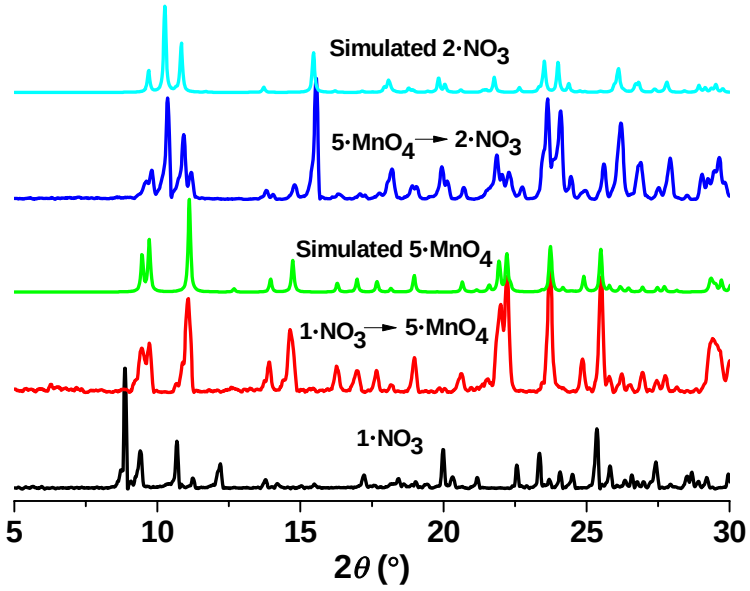

Figure S7. PXRD patterns indicating the reversibility for anion exchange.

Figure S8. The release of MnO_4^- by immersing **5·MnO₄** sample in a saturated water solution of KNO_3.

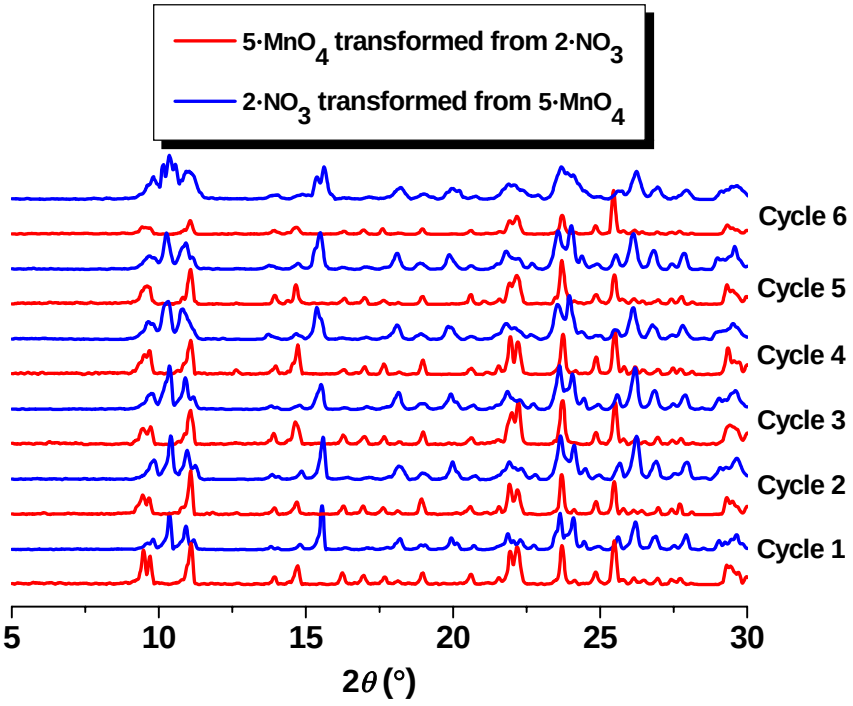

(a)

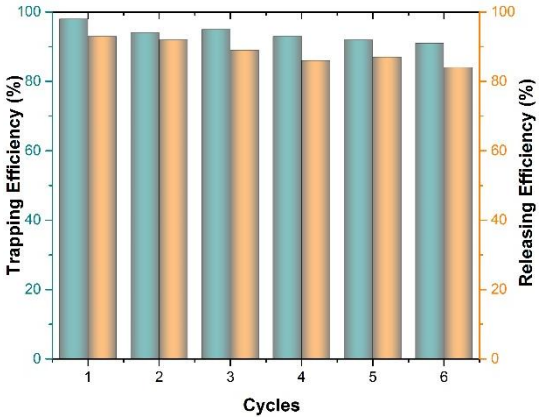

(b)

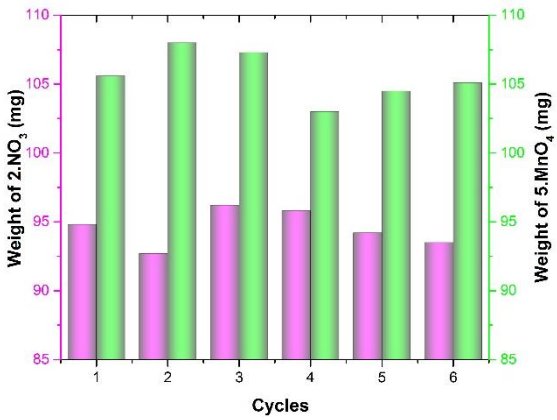

(c)

Figure S9. (a) PXRD patterns indicating the reversibility and reusability for anion exchange. (b) Trapping and releasing efficiencies in serial recycle tests. (c) The weight of **2·NO$_3$** and **5·MnO$_4$** samples in serial recycle tests.

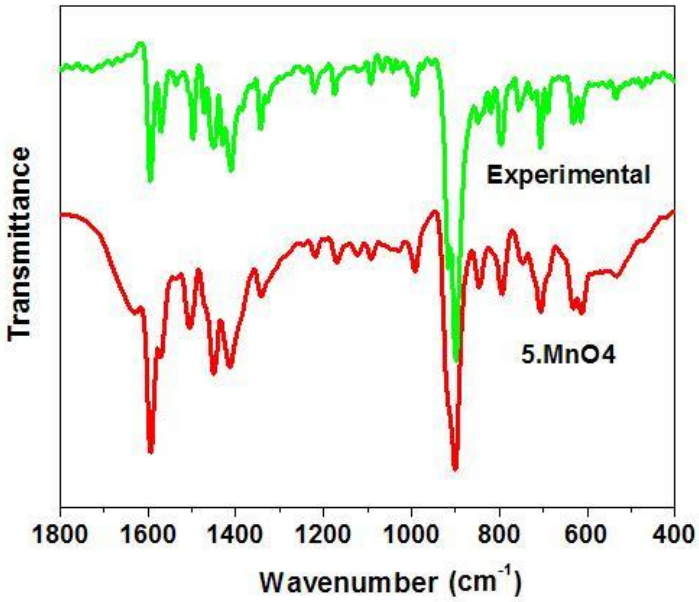

(a)

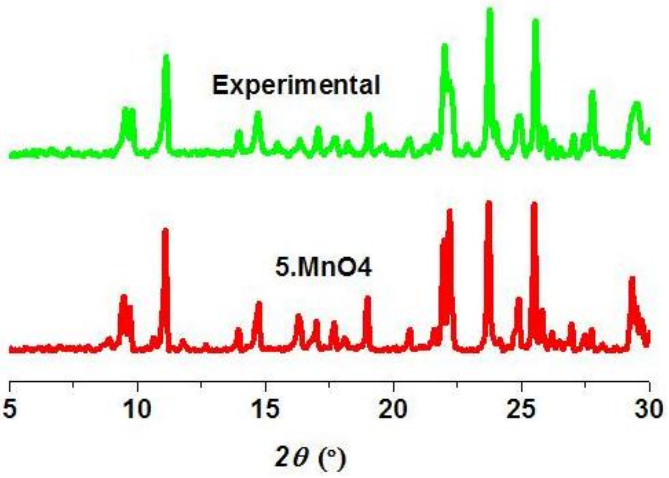

(b)

Figure S10. (a) FT-IR and (b) PXRD characterization of the anion-exchange product for shortest time of adsorption saturation.

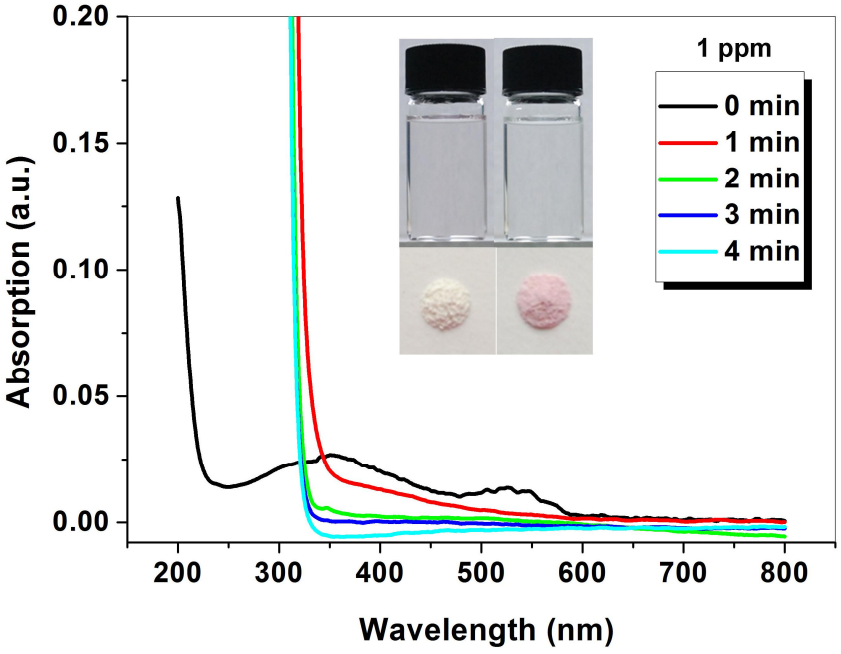

Figure S11. UV-Vis spectra and photos of the solution (inset: solid sample in detection limit experiment).

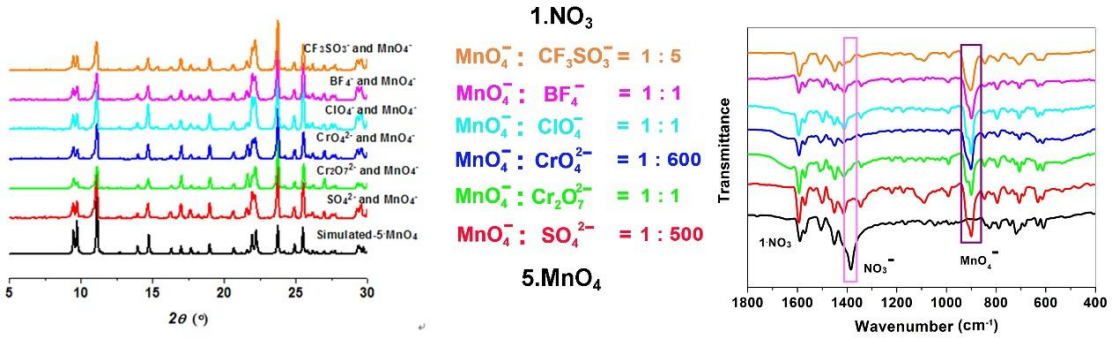

(a)

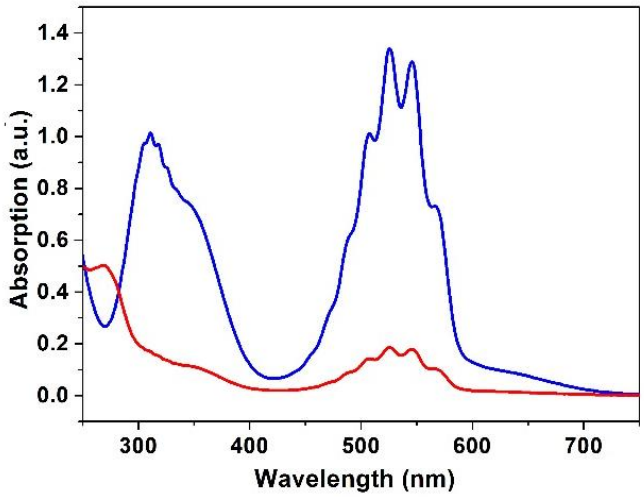

(b)

Figure S12. (a) PXRD and FT-IR characterization for selective anion exchange experiments. (b) UV-Vis spectra of the mixture solution containing $KMnO_4$ and the competing anions (CrO_4^{2-}, 100-fold; SO_4^{2-}, 100-fold; $CF_3SO_3^-$, 5-fold; ClO_4^-, 1-fold; BF_4^-, 1-fold; $Cr_2O_7^{2-}$, 1-fold) before and after anion exchange.

Table S1. Crystallographic Data and Structural Refinement Details for **1·NO_3**, **2·NO_3**, **3·NO_3·MnO_4**, **4·MnO_4** and **5·MnO_4**.

Compound reference	**1·NO_3**	**2·NO_3**	**3·NO_3·MnO_4**	**4·MnO_4**	**5·MnO_4**
Chemical formula	$C_{19}H_{17}AgN_8O_4$	$C_{17}H_{12}AgN_7O_3$	$C_{18}H_{13.5}AgMn_{0.84}N_{6.66}O_{3.84}$	$C_{18}H_{13.5}AgMnN_{6.5}O_4$	$C_{17}H_{12}AgMnN_6O_4$
Formula mass	529.28	470.21	538.70	547.66	527.14
Crystal system	monoclinic	monoclinic	monoclinic	monoclinic	monoclinic
a (Å)	10.45578(18)	9.7608(11)	10.2824(9)	10.2630(5)	9.3008(3)
b (Å)	14.5262(2)	18.2332(13)	14.8893(10)	14.9415(7)	18.1909(3)
c (Å)	14.2658(3)	10.4565(14)	14.3004(13)	14.3242(8)	11.4385(3)
β (°)	105.0179(19)	110.843(14)	103.428(9)	103.092(5)	108.077(3)
Unit cell volume ($Å^3$)	2092.74(6)	1739.2(3)	2129.5(3)	2139.45(19)	1839.75(8)
Temperature (K)	294(2)	294(2)	294(2)	294(2)	294(2)
Space group	$P2_1/n$	$P2_1/n$	$P2_1/n$	$P2_1/n$	$P2_1/n$
Z	4	4	4	4	4
Absorption coefficient, μ (mm^{-1})	1.008	1.195	1.460	1.543	1.789
No. of reflections measured	8857	6119	9064	8113	5281
No. of independent reflections	3683	3059	3950	3715	3184
R_{int}	0.0218	0.0334	0.0507	0.0380	0.0227
Final R_1 values ($I > 2\sigma(I)$)	0.0332	0.0495	0.0680	0.0737	0.0334
Final $wR(F^2)$ values ($I > 2\sigma(I)$)	0.0820	0.1080	0.1933	0.2140	0.0694
Final R_1 values (all data)	0.0438	0.0690	0.0838	0.1009	0.0433
Final $wR(F^2)$ values (all data)	0.0882	0.1147	0.2161	0.2310	0.0749
Goodness of fit on F^2	1.057	1.158	1.045	1.077	1.080

Table S2. Comparison of the Structural Features for L^{243} Ligands in **1·NO_3**, **2·NO_3**, **3·NO_3·MnO_4**, **4·MnO_4** and **5·MnO_4**.

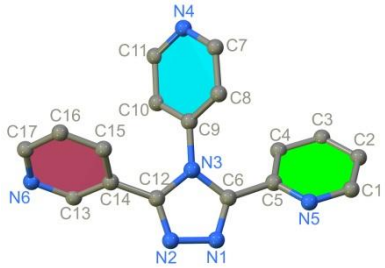

	1·NO_3	**2·NO_3**	**3·NO_3·MnO_4**	**4·MnO_4**	**5·MnO_4**
Conformation for L^{243}	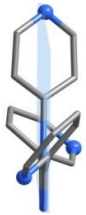	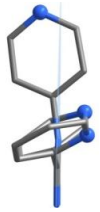			
Distortion of 2-Pyridyl Ring[a]	–44.3	+112.9	–47.3	+46.8	–97.4
Distortion of 3-Pyridyl Ring[b]	–59.0	–119.2	–53.8	+54.4	112.9
Dihedral Angle[c]	43.5	69.3	46.4	47.0	83.0
Dihedral Angle[d]	56.8	63.0	52.4	51.9	62.3

[a] Distortion angle of N1–C6–C5–N5. [b] Distortion angle of N2–C12–C14–C13. [c] Between 2-pyridyl and triazolyl. [d] Between 3-pyridyl and triazolyl.

Table S3. Comparison of the Structural Features for Host Coordination Frameworks in **1·NO_3**, **2·NO_3**, **3·NO_3·MnO_4**, **4·MnO_4** and **5·MnO_4**.

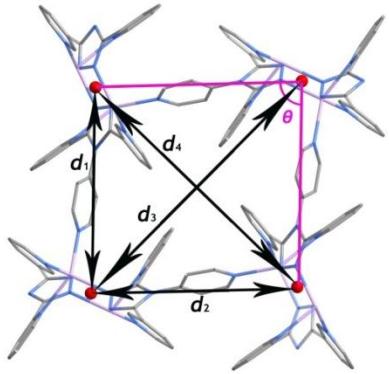

	1·NO_3	**2·NO_3**	**3·NO_3·MnO_4**	**4·MnO_4**	**5·MnO_4**
	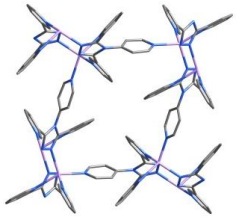	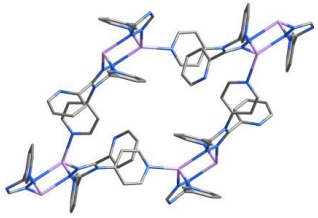	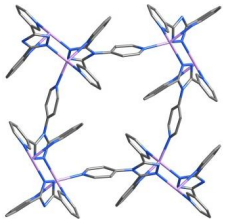	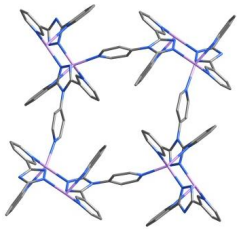	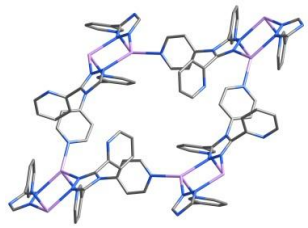
d_1 (Å)	12.26	10.78	10.77	10.81	10.98
d_2 (Å)	10.57	10.78	10.77	10.81	10.98
d_3 (Å)	14.55	18.23	14.89	14.94	18.19
d_4 (Å)	15.36	11.49	15.55	15.62	12.30
θ (°)	93.15	64.43	92.50	92.54	68.14

Table S4. UV-Vis Data for MnO_4^- Trapping with **1·NO₃** in Different Molar Ratios at 298 K or 353 K.

1·NO₃ : KMnO₄ = 1 : 1 (298 K)										
Time (min)	**1·NO₃** (mmol)	**1·NO₃** (g)	$KMnO_4$ (mmol)	$KMnO_4$ (g)	Exchange Ratio (%)	Exchange Capability ($mol \cdot mol^{-1}$)	Exchange Capability ($mg \cdot g^{-1}$)	Concentration of MnO_4^- ($mmol \cdot L^{-1}$)	Initial Absorbance Intensity of MnO_4^-	Absorbance Intensity of MnO_4^-
0	0.10	0.0529	0.10	0.0158	0.00	0.00	0.00	10.00	1.134	1.134
32	0.10	0.0529	0.10	0.0158	7.50	0.07	22.39	9.25	1.134	1.049
64	0.10	0.0529	0.10	0.0158	11.11	0.11	33.19	8.89	1.134	1.008
96	0.10	0.0529	0.10	0.0158	13.32	0.13	39.77	8.67	1.134	0.983
128	0.10	0.0529	0.10	0.0158	14.46	0.14	43.19	8.55	1.134	0.970
160	0.10	0.0529	0.10	0.0158	16.67	0.17	49.78	8.33	1.134	0.945
192	0.10	0.0529	0.10	0.0158	18.87	0.19	56.36	8.11	1.134	0.920
224	0.10	0.0529	0.10	0.0158	31.75	0.32	94.82	6.83	1.134	0.774
232	0.10	0.0529	0.10	0.0158	33.60	0.34	100.35	6.64	1.134	0.753
264	0.10	0.0529	0.10	0.0158	47.09	0.47	140.65	5.29	1.134	0.600
280	0.10	0.0529	0.10	0.0158	66.05	0.66	197.27	3.40	1.134	0.385
304	0.10	0.0529	0.10	0.0158	76.28	0.76	227.83	2.37	1.134	0.269
344	0.10	0.0529	0.10	0.0158	94.89	0.95	283.40	0.51	1.134	0.058
376	0.10	0.0529	0.10	0.0158	97.27	0.97	290.51	0.27	1.134	0.031
400	0.10	0.0529	0.10	0.0158	99.38	0.99	296.83	0.06	1.134	0.007
432	0.10	0.0529	0.10	0.0158	**99.74**	1.00	**297.89**	0.03	1.134	0.003

$1{\cdot}NO_3$: $KMnO_4$ = 2 : 1 (298 K)										
Time (min)	**$1{\cdot}NO_3$** (mmol)	**$1{\cdot}NO_3$** (g)	$KMnO_4$ (mmol)	$KMnO_4$ (g)	Exchange Ratio (%)	Exchange Capability ($mol{\cdot}mol^{-1}$)	Exchange Capability ($mg{\cdot}g^{-1}$)	Concentration of MnO_4^- ($mmol{\cdot}L^{-1}$)	Initial Absorbance Intensity of MnO_4^-	Absorbance Intensity of MnO_4^-
0	0.20	0.1058	0.10	0.0158	0.00	0.00	0.00	10.00	1.126	1.126
8	0.20	0.1058	0.10	0.0158	16.52	0.08	24.67	8.35	1.126	0.940
16	0.20	0.1058	0.10	0.0158	29.40	0.15	43.90	7.06	1.126	0.795
24	0.20	0.1058	0.10	0.0158	30.11	0.15	44.96	6.99	1.126	0.787
32	0.20	0.1058	0.10	0.0158	33.93	0.17	50.66	6.61	1.126	0.744
48	0.20	0.1058	0.10	0.0158	37.39	0.19	55.84	6.26	1.126	0.705
56	0.20	0.1058	0.10	0.0158	40.41	0.20	60.35	5.96	1.126	0.671
64	0.20	0.1058	0.10	0.0158	41.83	0.21	62.47	5.82	1.126	0.655
80	0.20	0.1058	0.10	0.0158	44.76	0.22	66.84	5.52	1.126	0.622
96	0.20	0.1058	0.10	0.0158	48.85	0.24	72.95	5.12	1.126	0.576
112	0.20	0.1058	0.10	0.0158	52.49	0.26	78.38	4.75	1.126	0.535
128	0.20	0.1058	0.10	0.0158	52.66	0.26	78.65	4.73	1.126	0.533
144	0.20	0.1058	0.10	0.0158	55.06	0.28	82.23	4.49	1.126	0.506
160	0.20	0.1058	0.10	0.0158	60.57	0.30	90.45	3.94	1.126	0.444
176	0.20	0.1058	0.10	0.0158	67.05	0.34	100.13	3.29	1.126	0.371
192	0.20	0.1058	0.10	0.0158	69.01	0.35	103.05	3.10	1.126	0.349
208	0.20	0.1058	0.10	0.0158	76.73	0.38	114.59	2.33	1.126	0.262
224	0.20	0.1058	0.10	0.0158	91.21	0.46	136.21	0.88	1.126	0.099
240	0.20	0.1058	0.10	0.0158	97.69	0.49	145.89	0.23	1.126	0.026
256	0.20	0.1058	0.10	0.0158	99.02	0.50	147.88	0.10	1.126	0.011
264	0.20	0.1058	0.10	0.0158	99.56	0.50	148.68	0.04	1.126	0.005
336	0.20	0.1058	0.10	0.0158	**99.82**	0.50	**149.07**	0.02	1.126	0.002

$1{\cdot}NO_3$: $KMnO_4$ = 4 : 1 (298 K)										
Time (min)	**$1{\cdot}NO_3$** (mmol)	**$1{\cdot}NO_3$** (g)	$KMnO_4$ (mmol)	$KMnO_4$ (g)	Exchange Ratio (%)	Exchange Capability ($mol{\cdot}mol^{-1}$)	Exchange Capability ($mg{\cdot}g^{-1}$)	Concentration of MnO_4^- ($mmol{\cdot}L^{-1}$)	Initial Absorbance Intensity of MnO_4^-	Absorbance Intensity of MnO_4^-
0	0.40	0.2116	0.10	0.0158	0.00	0.00	0.00	10.00	1.101	1.101
8	0.40	0.2116	0.10	0.0158	11.35	0.03	8.48	8.86	1.101	0.976
16	0.40	0.2116	0.10	0.0158	17.89	0.04	13.36	8.21	1.101	0.904
24	0.40	0.2116	0.10	0.0158	19.26	0.05	14.38	8.07	1.101	0.889
32	0.40	0.2116	0.10	0.0158	27.97	0.07	20.89	7.20	1.101	0.793
40	0.40	0.2116	0.10	0.0158	41.42	0.10	30.93	5.86	1.101	0.645
48	0.40	0.2116	0.10	0.0158	43.51	0.11	32.49	5.65	1.101	0.622
56	0.40	0.2116	0.10	0.0158	45.87	0.11	34.25	5.41	1.101	0.596
64	0.40	0.2116	0.10	0.0158	46.68	0.12	34.86	5.33	1.101	0.587
72	0.40	0.2116	0.10	0.0158	49.95	0.12	37.30	5.00	1.101	0.551
80	0.40	0.2116	0.10	0.0158	52.41	0.13	39.13	4.76	1.101	0.524
88	0.40	0.2116	0.10	0.0158	56.49	0.14	42.18	4.35	1.101	0.479
96	0.40	0.2116	0.10	0.0158	61.22	0.15	45.71	3.88	1.101	0.427
104	0.40	0.2116	0.10	0.0158	62.94	0.16	47.00	3.71	1.101	0.408
112	0.40	0.2116	0.10	0.0158	68.94	0.17	51.47	3.11	1.101	0.342
120	0.40	0.2116	0.10	0.0158	74.39	0.19	55.54	2.56	1.101	0.282
128	0.40	0.2116	0.10	0.0158	77.48	0.19	57.85	2.25	1.101	0.248
136	0.40	0.2116	0.10	0.0158	85.65	0.21	63.95	1.44	1.101	0.158
144	0.40	0.2116	0.10	0.0158	90.83	0.23	67.82	0.92	1.101	0.101
152	0.40	0.2116	0.10	0.0158	93.19	0.23	69.58	0.68	1.101	0.075
160	0.40	0.2116	0.10	0.0158	94.28	0.24	70.40	0.57	1.101	0.063
168	0.40	0.2116	0.10	0.0158	96.91	0.24	72.36	0.31	1.101	0.034
176	0.40	0.2116	0.10	0.0158	98.00	0.25	73.18	0.20	1.101	0.022

184	0.40	0.2116	0.10	0.0158	98.64	0.25	73.65	0.14	1.101	0.015
192	0.40	0.2116	0.10	0.0158	99.36	0.25	74.19	0.06	1.101	0.007
200	0.40	0.2116	0.10	0.0158	99.64	0.25	74.40	0.04	1.101	0.004
208	0.40	0.2116	0.10	0.0158	**99.73**	0.25	**74.47**	0.03	1.101	0.003

$1{\cdot}NO_3$: $KMnO_4$ = 1 : 1 (353 K)										
Time (min)	**$1{\cdot}NO_3$** (mmol)	**$1{\cdot}NO_3$** (g)	$KMnO_4$ (mmol)	$KMnO_4$ (g)	Exchange Ratio (%)	Exchange Capability ($mol{\cdot}mol^{-1}$)	Exchange Capability ($mg{\cdot}g^{-1}$)	Concentration of MnO_4^- ($mmol{\cdot}L^{-1}$)	Initial Absorbance Intensity of MnO_4^-	Absorbance Intensity of MnO_4^-
0	0.10	0.0529	0.10	0.0158	0.00	0.00	0.00	10.00	1.110	1.110
8	0.10	0.0529	0.10	0.0158	9.91	0.10	29.60	9.01	1.110	1.000
16	0.10	0.0529	0.10	0.0158	23.78	0.24	71.04	7.62	1.110	0.846
24	0.10	0.0529	0.10	0.0158	36.40	0.36	108.71	6.36	1.110	0.706
32	0.10	0.0529	0.10	0.0158	43.24	0.43	129.16	5.68	1.110	0.630
40	0.10	0.0529	0.10	0.0158	53.69	0.54	160.37	4.63	1.110	0.514
48	0.10	0.0529	0.10	0.0158	59.10	0.59	176.52	4.09	1.110	0.454
56	0.10	0.0529	0.10	0.0158	65.14	0.65	194.54	3.49	1.110	0.387
64	0.10	0.0529	0.10	0.0158	70.90	0.71	211.76	2.91	1.110	0.323
72	0.10	0.0529	0.10	0.0158	77.57	0.78	231.68	2.24	1.110	0.249
80	0.10	0.0529	0.10	0.0158	82.25	0.82	245.67	1.77	1.110	0.197
88	0.10	0.0529	0.10	0.0158	85.86	0.86	256.43	1.41	1.110	0.157
96	0.10	0.0529	0.10	0.0158	88.20	0.88	263.43	1.18	1.110	0.131
104	0.10	0.0529	0.10	0.0158	91.98	0.92	274.73	0.80	1.110	0.089
112	0.10	0.0529	0.10	0.0158	92.79	0.93	277.15	0.72	1.110	0.080
120	0.10	0.0529	0.10	0.0158	94.50	0.95	282.26	0.55	1.110	0.061
128	0.10	0.0529	0.10	0.0158	96.31	0.96	287.64	0.37	1.110	0.041
136	0.10	0.0529	0.10	0.0158	98.56	0.99	294.37	0.14	1.110	0.016
144	0.10	0.0529	0.10	0.0158	99.55	1.00	297.33	0.05	1.110	0.005
152	0.10	0.0529	0.10	0.0158	**99.64**	1.00	**297.60**	0.04	1.110	0.004

$1{\cdot}NO_3$: $KMnO_4$ = 2 : 1 (353 K)										
Time (min)	**$1{\cdot}NO_3$** (mmol)	**$1{\cdot}NO_3$** (g)	$KMnO_4$ (mmol)	$KMnO_4$ (g)	Exchange Ratio (%)	Exchange Capability ($mol{\cdot}mol^{-1}$)	Exchange Capability ($mg{\cdot}g^{-1}$)	Concentration of MnO_4^- ($mmol{\cdot}L^{-1}$)	Initial Absorbance Intensity of MnO_4^-	Absorbance Intensity of MnO_4^-
0	0.20	0.1058	0.10	0.0158	0.00	0.00	0.00	10.00	1.115	1.115
8	0.20	0.1058	0.10	0.0158	16.86	0.08	25.18	8.31	1.115	0.927
16	0.20	0.1058	0.10	0.0158	36.95	0.18	55.18	6.30	1.115	0.703
24	0.20	0.1058	0.10	0.0158	47.17	0.24	70.45	5.28	1.115	0.589
32	0.20	0.1058	0.10	0.0158	61.08	0.31	91.21	3.89	1.115	0.434
40	0.20	0.1058	0.10	0.0158	73.27	0.37	109.43	2.67	1.115	0.298
48	0.20	0.1058	0.10	0.0158	83.32	0.42	124.43	1.67	1.115	0.186
56	0.20	0.1058	0.10	0.0158	88.97	0.44	132.86	1.10	1.115	0.123
64	0.20	0.1058	0.10	0.0158	95.25	0.48	142.24	0.48	1.115	0.053
72	0.20	0.1058	0.10	0.0158	96.05	0.48	143.45	0.39	1.115	0.044
80	0.20	0.1058	0.10	0.0158	97.49	0.49	145.59	0.25	1.115	0.028
96	0.20	0.1058	0.10	0.0158	98.57	0.49	147.20	0.14	1.115	0.016
104	0.20	0.1058	0.10	0.0158	99.55	0.50	148.67	0.04	1.115	0.005
130	0.20	0.1058	0.10	0.0158	**99.82**	0.50	**149.07**	0.02	1.115	0.002

1·NO_3 : $KMnO_4$ = 4 : 1 (353 K)										
Time (min)	**1·NO_3** (mmol)	**1·NO_3** (g)	$KMnO_4$ (mmol)	$KMnO_4$ (g)	Exchange Ratio (%)	Exchange Capability ($mol \cdot mol^{-1}$)	Exchange Capability ($mg \cdot g^{-1}$)	Concentration of MnO_4^- ($mmol \cdot L^{-1}$)	Initial Absorbance Intensity of MnO_4^-	Absorbance Intensity of MnO_4^-
0	0.40	0.2116	0.10	0.0158	0.00	0.00	0.00	10.00	1.098	1.098
4	0.40	0.2116	0.10	0.0158	14.66	0.04	10.95	8.53	1.098	0.937
8	0.40	0.2116	0.10	0.0158	20.22	0.05	15.10	7.98	1.098	0.876
12	0.40	0.2116	0.10	0.0158	41.53	0.10	31.01	5.85	1.098	0.642
16	0.40	0.2116	0.10	0.0158	57.83	0.14	43.18	4.22	1.098	0.463
20	0.40	0.2116	0.10	0.0158	65.85	0.16	49.17	3.42	1.098	0.375
24	0.40	0.2116	0.10	0.0158	78.78	0.20	58.82	2.12	1.098	0.233
28	0.40	0.2116	0.10	0.0158	82.70	0.21	61.75	1.73	1.098	0.190
32	0.40	0.2116	0.10	0.0158	87.52	0.22	65.35	1.25	1.098	0.137
36	0.40	0.2116	0.10	0.0158	90.53	0.23	67.60	0.95	1.098	0.104
40	0.40	0.2116	0.10	0.0158	93.53	0.23	69.84	0.65	1.098	0.071
44	0.40	0.2116	0.10	0.0158	94.99	0.24	70.93	0.50	1.098	0.055
48	0.40	0.2116	0.10	0.0158	95.63	0.24	71.40	0.44	1.098	0.048
52	0.40	0.2116	0.10	0.0158	95.72	0.24	71.47	0.43	1.098	0.047
56	0.40	0.2116	0.10	0.0158	96.17	0.24	71.81	0.38	1.098	0.042
60	0.40	0.2116	0.10	0.0158	96.27	0.24	71.88	0.37	1.098	0.041
64	0.40	0.2116	0.10	0.0158	96.45	0.24	72.02	0.36	1.098	0.039
68	0.40	0.2116	0.10	0.0158	97.72	0.24	72.97	0.23	1.098	0.025
72	0.40	0.2116	0.10	0.0158	98.45	0.25	73.51	0.15	1.098	0.017
80	0.40	0.2116	0.10	0.0158	99.27	0.25	74.13	0.07	1.098	0.008
96	0.40	0.2116	0.10	0.0158	**99.64**	0.25	**74.40**	0.04	1.098	0.004
104	0.40	0.2116	0.10	0.0158	99.64	0.25	74.40	0.04	1.098	0.004
130	0.40	0.2116	0.10	0.0158	99.64	0.25	74.40	0.04	1.098	0.004

Table S5. Adsorption Capacity (Ads. Cap.) of MnO_4^- (0.1 mmol) in Water (10 mL) with Different Amounts of **1·NO₃** at 298 K and 353 K.

			UV-Vis			ICP		
Temp. (K)	Molar Ratio*	Time (min)	Anion Removal	Ads. Cap. ($mol \cdot mol^{-1}$)	Ads. Cap. ($mg \cdot g^{-1}$)	Anion Removal	Ads. Cap. ($mol \cdot mol^{-1}$)	Ads. Cap. ($mg \cdot g^{-1}$)
298	1 : 1	264	47.09%	0.47	140.65	46.21%	0.46	138.01
		432	99.74%	1.00	297.89	99.47%	0.99	297.10
	2 : 1	96	48.85%	0.24	72.95	48.67%	0.24	72.68
		336	99.82%	0.50	149.07	99.64%	0.50	148.81
	4 : 1	72	49.95%	0.12	37.30	48.50%	0.12	36.22
		208	99.73%	0.25	74.47	99.55%	0.25	74.33
353	1 : 1	32	43.24%	0.43	129.16	41.44%	0.41	123.78
		152	99.64%	1.00	297.60	99.55%	1.00	297.33
	2 : 1	24	47.17%	0.24	70.45	45.74%	0.23	68.31
		130	99.82%	0.50	149.07	99.64%	0.50	148.80
	4 : 1	12	41.53%	0.10	31.01	40.07%	0.10	29.92
		96	99.64%	0.25	74.40	99.36%	0.25	74.19

* The initial molar ratios of **1·NO₃** : MnO_4^-.

Table S6. Experimental Details for High-Throughput Crystallization Screening Based on Concentration-Gradient Design of the Starting Reagents.*

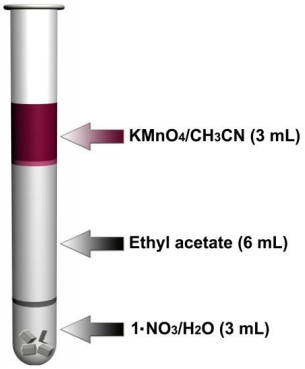

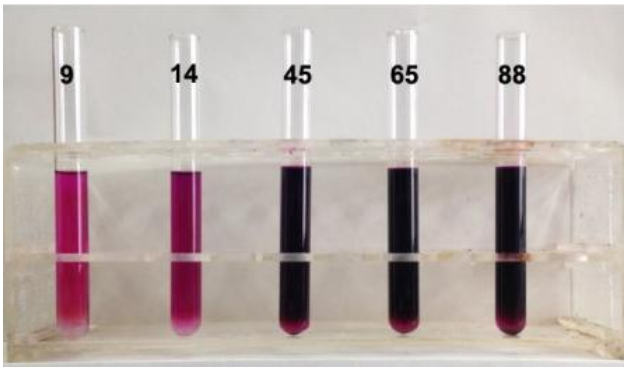

$KMnO_4$ (mmol) / **1·NO_3** (mmol)	0.01	0.02	0.04	0.08	0.12	0.16	0.20	0.24	0.28	0.32
0.01	**1**	**11**	**21**	**31**	**41**	**51**	**61**	**71**	**81**	**91**
0.02	**2**	**12**	**22**	**32**	**42**	**52**	**62**	**72**	**82**	**92**
0.03	**3**	**13**	**23**	**33**	**43**	**53**	**63**	**73**	**83**	**93**
0.04	**4**	**14**	**24**	**34**	**44**	**54**	**64**	**74**	**84**	**94**
0.05	**5**	**15**	**25**	**35**	**45**	**55**	**65**	**75**	**85**	**95**
0.06	**6**	**16**	**26**	**36**	**46**	**56**	**66**	**76**	**86**	**96**
0.07	**7**	**17**	**27**	**37**	**47**	**57**	**67**	**77**	**87**	**97**
0.08	**8**	**18**	**28**	**38**	**48**	**58**	**68**	**78**	**88**	**98**
0.09	**9**	**19**	**29**	**39**	**49**	**59**	**69**	**79**	**89**	**99**
0.10	**10**	**20**	**30**	**40**	**50**	**60**	**70**	**80**	**90**	**100**

* The colored cells in this Table indicate that qualified crystals can be picked out for SC-XRD measurement (grey: **1·NO_3**; purple: **2·NO_3**; green: **3·NO_3·MnO_4** + **4·MnO_4**; blue: **5·MnO_4**). The red numbers are samples reported in the text.